Anti-Stokes signal conversion in the higher-order modes of photonic crystal fiber

JINHUI YUAN[*], XINZHU SANG, CHONGXIU YU, XIANGJUN XIN, GUIYAO ZHOU[a], SHUGUANG LI[a], LANTIAN HOU[a]

Key Laboratory of Information Photonics and Optical Communications (Beijing University of Posts and Telecommunications), Ministry of Education, P.O. Box163 (BUPT), 100876 Beijing, China
[a]Institute of Infrared Optical Fibers and Sensors, College of Information Science and Engineering, Yanshan University, Qinhuangdao 066004, China

With the photonic crystal fiber (PCF) with the zero dispersion wavelengths of second-order and third-order mode around 775 nm and 770 nm designed and fabricated in our lab, the anti-Stokes signals at 575 nm and 570 nm are efficiently generated in the second-order and third-order mode by Ti: sapphire laser with working wavelength of 845 nm and pulse width of 200 fs. In the experiment, most of pump energy is coupled into the higher-order modes by adjusting the angle between input pump and principal axis of fiber to be 25°and 30°, and the phase-matching four-wave mixing (FWM) takes place remarkably.

1. Introduction

Photonic crystal fibers (PCFs) [1,2] have attracted extensive attentions because of unique characteristics of guiding light such as endlessly single mode transmission, controlled dispersion [3,4], and highly nonlinearity [5], and so on. The optical confinement and nonlinear effects of PCFs can be enhanced through increasing the diameters of cladding holes as well as reducing the size of core [6-8]. Moreover, with the pump femtosecond lasers operating around the zero-dispersion wavelength, generation of anti-Stokes signal based on phase-matching four wave-mixing (FWM) is remarkable [9-15]. The process of efficient generation of anti-Stokes signal has been widely investigated to generate short-wavelength radiation for high-resolution imaging, direct excitation of electronic molecular transitions, multi-photon ionization, as well as preparation of vibrational wave packets [16], and so on.

M.L.Hu et al experimentally demonstrated the vectorial nonlinear-optical processes in multimode PCFs, and analyzed and controlled the frequency transformations of ultrashort laser pulses in the fundamental and second-order modes of PCFs based on the phase-matching condition [15]. W. Wang et al achieved a higher efficiency anti-Stokes signal conversion of femtosecond pulses in the second-order mode using a special PCF with two zero dispersion wavelengths [11]. In this letter, the high efficient conversions of anti-Stokes signals at 575 nm and 570 nm are presented both theoretically and experimentally based on the second-order and third-order mode with zero dispersion wavelengths 775 nm and 770 nm. The phase-matched FWM dominates the process of frequency conversion.

2. The properties of PCF and experimental set up

The cross-section of PCF designed and fabricated in our lab is shown in Fig.1. The structure parameters are as follows: the average hole diameters d=2.6 μm, hole to hole pitch Λ=3.2 μm, the average core diameter D=2.8 μm, and the air filling fraction f=0.8. The PCF fabricated with the improved stack-and-draw technique shows some degree of deformation such as the expanding and decreasing of cladding holes, the elliptical shape core, and so on due to the restriction of arts and crafts including the fluctuation of temperature and no-symmetrical distribution of tension. Not only the fundamental mode, but also second-order and third-order mode are propagated along the axis direction because of larger index contrast between core and cladding region.
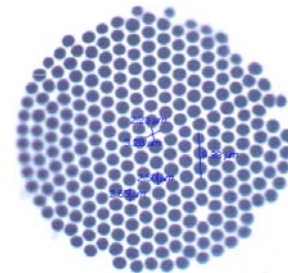
Fig. 1. Cross-section of PCF used in the experiment.

Multi-pole method (MPM) [17] has been used to analyze the properties of waveguide mode in PCF. The effective index curves of different order modes are shown in Fig.2. The difference of effective index between the second-order and third-order mode is small in the wavelength range of 0.4 to1.25 μm, indicating the similar characteristics of dispersion and mode. The effective index of fundamental mode decreases from 1.468 to 1.41 in the wavelength range of 0.4 to 1.8 μm, while the corresponding effective indices of second-order and third-order mode decrease from 1.466 to 1.41 in the wavelength range of 0.4 to 1.25 μm, showing higher loss and narrower transmission bandwidth compared to the fundamental mode. As seen from Fig. 2 (b), (c) and (d), the fundamental mode shows a Gauss-like shape which reaches its maximum at the center of the fiber core and monotonically decreasing with the distance from the center, for second-order and third-order mode, and some deformations emerge.

(a)

(b)   *(c)*   *(d)*
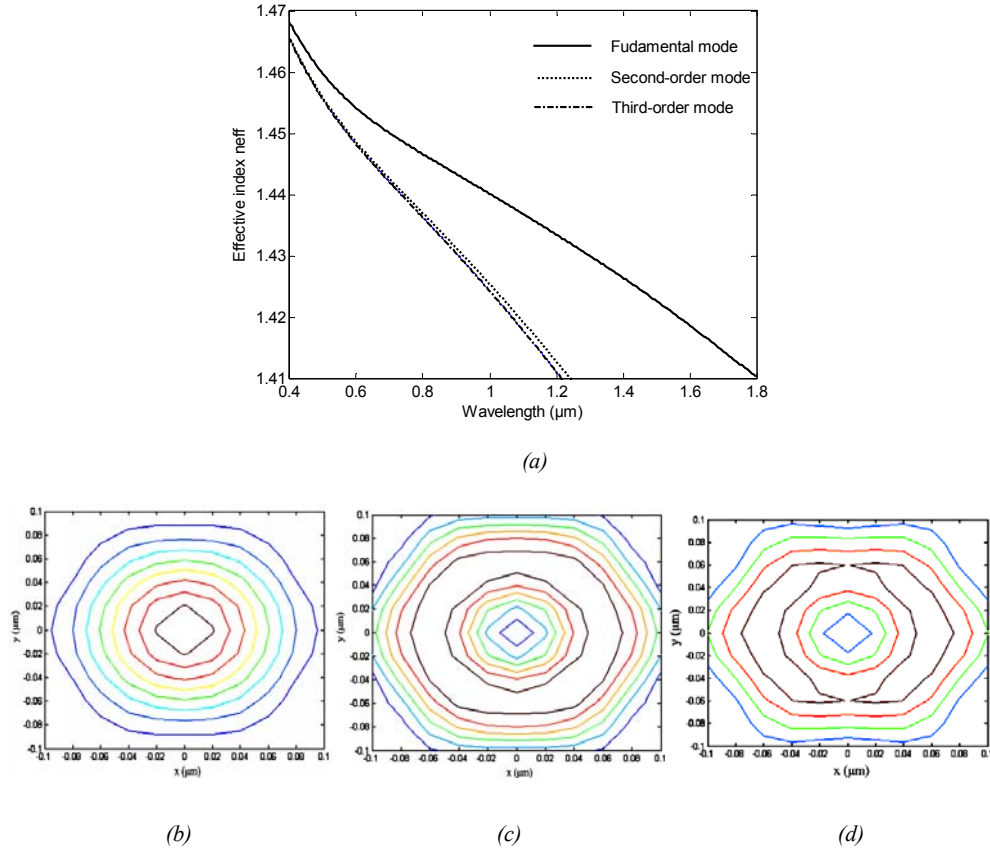
Fig. 2. (a) The effective refractive indices of fundamental (solid line), second-order (shorter dash line) and third-order (longer dash line)   mode   as a function of wavelength, and (b), (c) and (d) show the two dimension field distributions of fundamental mode, second order-mode and third-order mode.

Fig. 3 (a) are the group-velocity dispersions D of the fundamental, second-order and third-order mode of PCF calculated as a function of wavelength, and the material dispersion is considered from Sellmeyer equation. The wave vector mismatch $k = \Delta k_m + \Delta k_w + \Delta k_{NL}$ results from the silica material Δk_m and the waveguide Δk_w. The large mismatch can be compensated with the waveguide contribution Δk_w due to larger contrast of core-cladding index, while Δk_{NL} can compensate the residual mismatch of $\Delta k_m + \Delta k_w$.

In order to achieve high energy transfer from pump to signals in degenerate FWM, the phase-matching condition $k = \beta(\omega_S) + \beta(\omega_a) - 2\beta(\omega_p) + 2n_2 \omega_p P_p / (c A_{eff}) = 0$ has to be satisfied where $\beta(\omega_p)$, $\beta(\omega_S)$, and $\beta(\omega_a)$ are the propagation constants of pump, Stokes and anti-Stokes signals in the PCF, ω_p, ω_S, and ω_a correspond to the angle frequencies of pump, Stokes and anti-Stokes signals, P_p is the pump power, n_2 is the nonlinear refractive index, c is the vacuum light velocity, and A_{eff} is the effective mode field area. Fig. 3 (b) shows the phase-mismatching cases of the fundamental, second-order and third-order mode.

(a) *(b)*
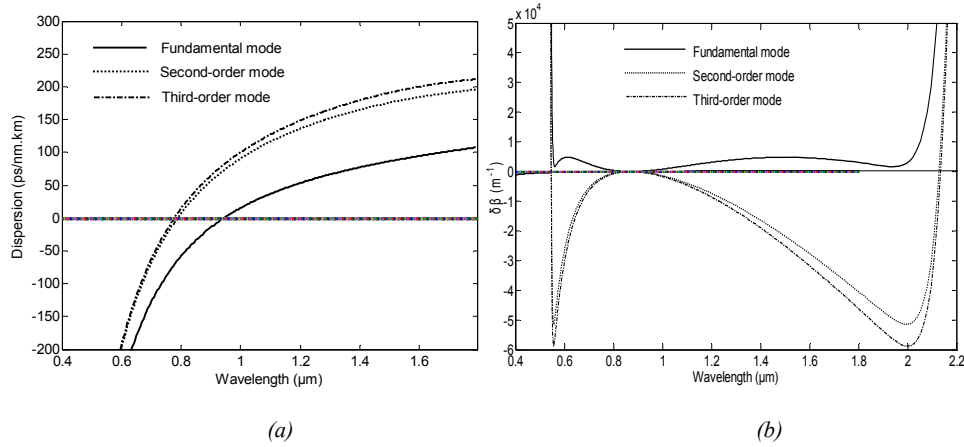
Fig. 3. (a) The group-velocity dispersion D of the fundamental (solid line), second-order (shorter dash line) and third-order (longer dash line) mode as a function of wavelength. (b) The phase-mismatching δβ of three kinds of mode as a function of wavelength.

In Fig. 3 (a), the zero-dispersion wavelengths of fundamental mode, second-order and third-order mode are located at 950 nm, 775 nm and 770 nm, respectively, and the discrepancy of dispersion curves between the second-order and third-order mode is small due to less index difference. Moreover, the absolute coupling between the two kinds of modes will not occur because of larger mismatching of wave-vectors, and it is possible that the phase-matching conditions are achieved. As shown in Fig. 3 (b), the anti-Stokes signals will emerge at 575 nm and 570 nm with Stokes signals rising at 2090 nm and 2100 nm. The configuration of experimental setup is shown in Fig. 4.
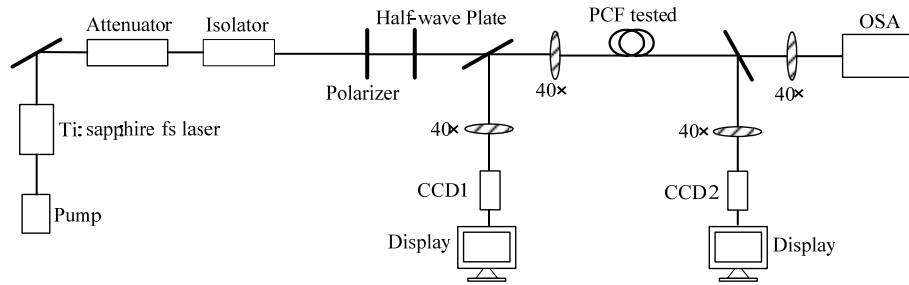
Fig. 4. The configuration of experimental setup.

In the experiment, the pump laser is a mode-locked Ti: sapphire laser with adjustable work wavelength from 750 to 950 nm, wavelength, emitting a 200 fs pulse train at the repetition rate of 76 MHz. The highest average input power is 300 mW and an optical isolator served to protect the laser oscillator from radiation backreflected from the focusing optics and the fiber. A polarizer was used to purify the input polarization, and a rotating half-wave plate was put between the polarizer and the fiber input end to adjust the input polarization. The light energy is mainly coupled into the second-order and third-order modes (as shown in Fig. 2 (c) and (d)) through exactly adjusting the angles between input light beam and fiber axis to be 25° and 30°. A 40x anti-reflection coated aspheric singlet lens was used to couple laser radiation into the PCF with a length of 45 cm. The input coupling efficiency was about 40 %. The CCD1 and CCD 2 are used for watching the coupling state of input light and output mode fields, and an optical spectrum analyzer (OSA) with the measurement scope from 200 to 1200 nm and a resolution of 0.1 nm is used to observe the output spectrum.

3. Results and discussion

In the experimental process, the working wavelength and input power of pump are adjusted reasonably, and the second-order and third-order mode are excited selectively to achieve phase-matching FWM. As shown in Fig. 5, the output spectrum of anti-Stoke signals are consistent with

the phase-matching cases of Fig. 3 (b).

(a)

(b)
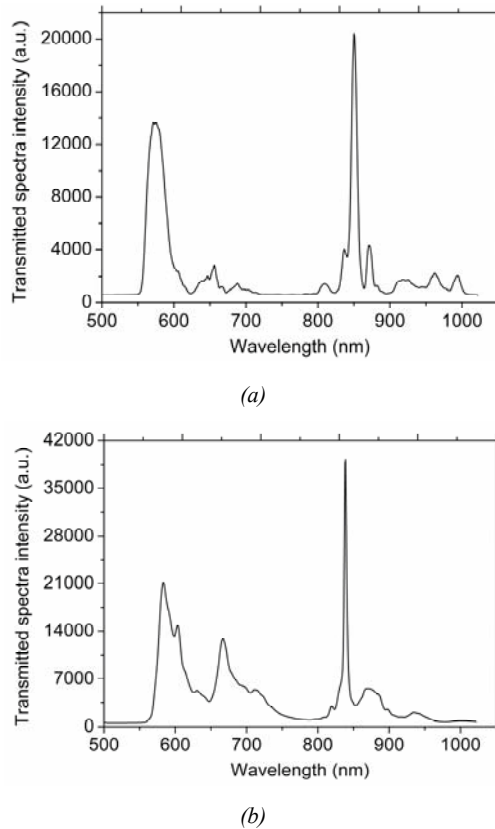
Fig. 5. The anti-stokes signal conversions in (a) second-order mode and (b) the third-order mode.

In Fig. 5 (a), while the input pump is at the anomalous dispersion region of 845 nm and the average power of 240 mW is mainly coupled into the second-order mode, the remarkable anti-Stokes signal at 575 nm is generated, and the ratio of output spectra intensities between anti-Stokes signal and residual pump is about 0.65. Considering higher loss of the third-order mode, the input average power is increased to 280 mW and the pump wavelength is kept constant. As shown in Fig.5 (b), the anti-Stokes signal is given to rise at 570 nm, and the corresponding ratio of output spectra intensities is about 0.55. Comparing with Fig. 5 (b) and (a), it is found that the ratio of output spectra intensities based on the third-order mode is lower than the one based on the second-order mode, and the main reason is considered to be larger phase-mismatching and higher loss of third-order mode.

When the phase-matching condition is well satisfied along the fiber length, the Raman effects may have an important influence on frequency conversion within the gain spectrum of Raman. Moreover, another wave peak is emerging at 675 nm in the output spectra, as shown in Fig. 5 (b), and the possible reason is considered that other polarization state of the third-order mode due to core birefringence emerges and a part of pump power is coupled into the corresponding polarization modes.

Moreover, the Stokes components corresponding to the phase-matching wavelengths of 2090 nm and 2100 nm (as shown in Fig. 3 (b)) aren't observed, and two main reasons are considered. First, the spectrum of Stokes components is beyond the measurement range of OSA. Second, considering the higher conversion efficiency of anti-Stokes signals and possible hundreds of dB/m transmission loss of fibers, it is possible that the total energy of these Stokes components is depleted at the output of fiber. It is worth noting that the signal interference can be depressed due to lower higher depletion of Stokes components, and better output quality of anti-Stokes signal can be obtained.

4. Conclusions

The remarkable anti-Stokes signals based on the second-order and third-order mode of PCF are generated through adjusting the angle between input pump and fiber principal axis and coupling the fs pulse into the PCF. The phase-matching FWM is shown, the reasons for discrepancies between experimental and theoretical results are analyzed, and the influences of other factors on the signal conversion are discussed.

References

[1] J. C. Knight, P. S. J. Russell, Science **296**, 276 (2002).
[2] P. S. J. Russell, Science **299,** 358 (2003).
[3] B. Kuhlmey, G. Renversez, D. Maystre, Appl. Opt. **42,** 634 (2003).
[4] L. P. Shen, W. P. Huang, S. S. Jian, J. Lightw. Technol. **21,** 1644 (2003).
[5] X. Z. Sang, P. K. Chu, C. X. Yu, Opt. and Quantum Electron. **37,** 965 (2005).
[6] F. Poli, A. Cucinotta, S. Selleri, A. H. Bouk, IEEE Photon. Technol. Lett. **16,** 1065 (2004).
[7] A. B. Fedotov, A. M. Zheltikov, A. P. Tarasevitch, D. von der Linde, Appl. Phys. B **73,** 181 (2001).
[8] J. M. Dudley, L. Provino, N. Grossard, H. Maillotte, R. S. Windeler, B. J. Eggleton, S. Coen, J. Opt. Soc. Am. B **19,** 765 (2002).
[9] W. H. Reeves, D. V. Skryabin, F. Biancalana, J. C. Knight, P. S. J. Russell, F. G. Omenetto, A. Efimov, A. J. Taylor, Nature **424,** 511 (2003).
[10] S. O. Konorov, E. E. Serebryannikov, A. M.

Zheltikov, Opt. Lett. **29,** 1545 (2004).

[11] W. Wang, F. Gao, L. T. Hou, G. Y. Zhou, Chin. Phys. Lett. **25,** 2055 (2008).

[12] T. V. Andersen, K. M. Hilligsøe, C. K. Nielsen, Opt . Express. **12,** 4113 (2004).

[13] M. L. Hu, C. Y. Wang, L. Chai, Opt, Express. **12,** 1232 (2004).

[14] S. G. Li, L. T. Hou, Y. L. Ji, G. Y. Zhou, Chin. Phys. Lett. **20,** 1300 (2003).

[15] M. L. Hu, C. Y. Wang, Y. J. Song, Y. F. Li, L. Chai, Opt. Exp. **14**, 1189 (2006).

[16] A. H. Zewail, Science **242,** 1645 (1988).

[17] T. P. White, B. T. Kuhlmey, R. C. McPhedran, D. Maystre, G. Renversez, C. Martijn de Sterke, L. C. Botten, J. Opt. Soc. B. **19,** 2322 (2002).

[*]Corresponding author: yuanjinhui81@163.com